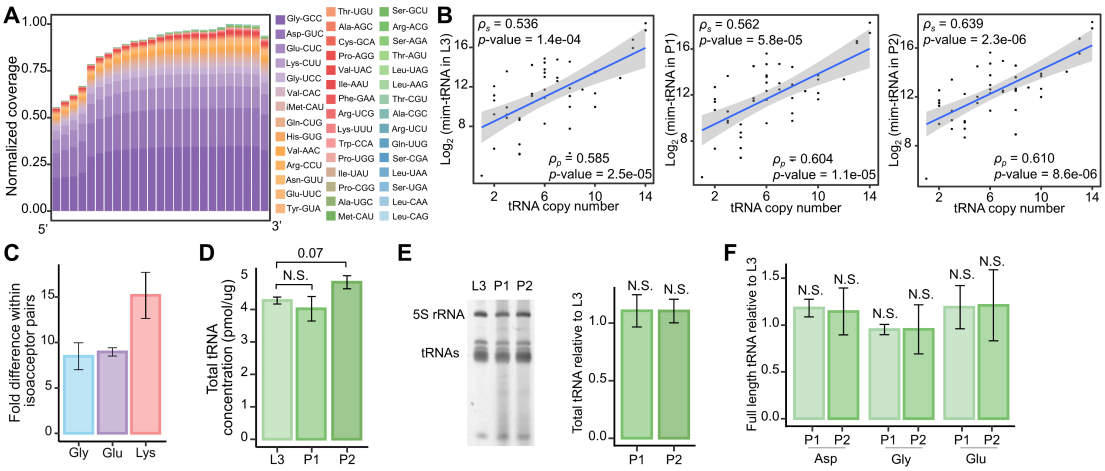

Supplemental Figure S1. mim-tRNAseq reveals a stable expression level of tRNAs during the larva-to-pupa transition

(A) Metagene analysis of mim-tRNAseq read coverage along the tRNA length. Each *x*-axis bin represents 4% of tRNA length. The *y*-axis values were computed by pooling all the 8 libraries of this study, and normalized to the peak value. Each color represents a unique group of nuclear-encoded tRNAs with the same anticodon, ordered according to the *y*-axis values.

(B) Scatterplots show the correlations between tRNA abundances (RPM) and tRNA gene copy numbers in libraries of L3, P1 and P2, respectively. Each dot represents a group of tRNAs sharing a unique anticodon.

(C) Fold differences within each pair of isoacceptor tRNAs: $tRNA^{Gly\text{-}GCC}$/$tRNA^{Gly\text{-}UCC}$, $tRNA^{Glu\text{-}CUC}$/$tRNA^{Glu\text{-}UUC}$ and $tRNA^{Lys\text{-}CUU}$/$tRNA^{Lys\text{-}UUU}$. For each pair, the former one has a greater number of gene copies. Errorbars represent SEM computed from 8 different libraries.

(D) Absolute quantification of total tRNA concentrations using mim-tRNAseq with a spike-in control (see Materials and Methods for details). Errorbars represent SEM computed from different libraries at each stage. N.S. denotes a Student's *t*-test $p > 0.1$.

(E) Relative quantification of total tRNAs using SYBR-gold staining. Error bars represent SD computed from two independent experiments.

(F) Relative quantification of $tRNA^{AspGUC}$, $tRNA^{GlyGCC}$ and $tRNA^{GluCUC}$ using Northern blot (Figure 2H). Error bars represent SD computed from three independent experiments.

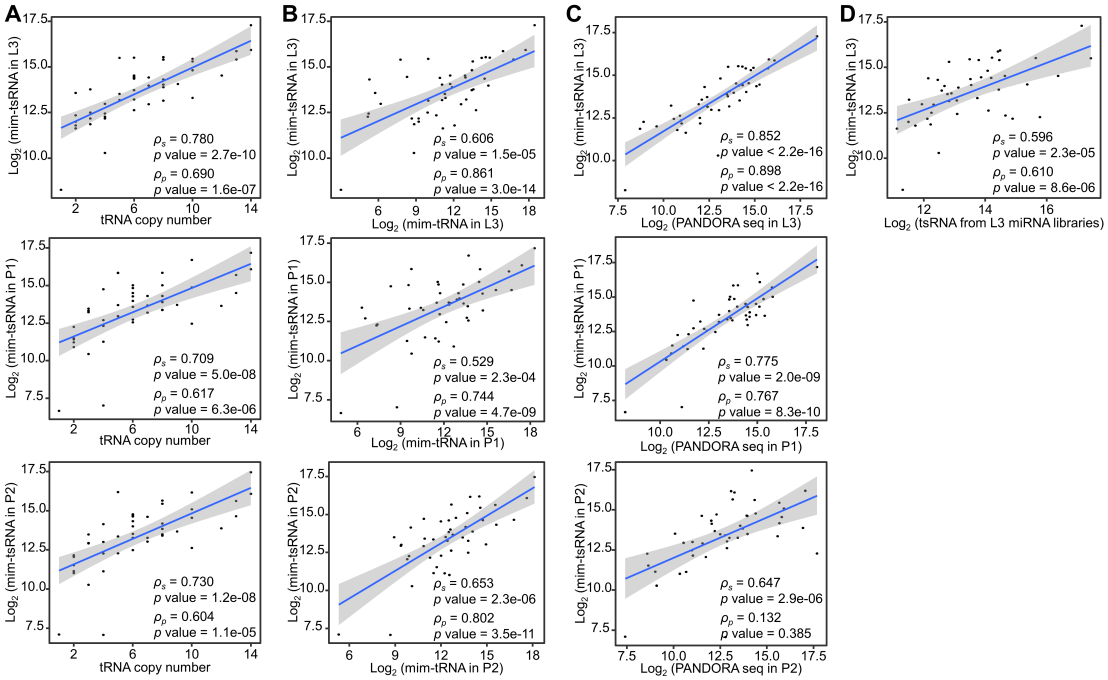

Supplemental Figure S2. mim-tRNA/tsRNA-seq detects a reliable correlation between tsRNA and tRNA levels in larvae and early pupae of *Drosophila*

(A-C) Scatterplots showing that at each developmental stage, tsRNA abundances (RPM) measured by mim-tsRNA-seq were correlated (Pearson's correlation) with tRNA gene copy numbers (A), tRNA abundances measured by mim-tRNA-seq (B), and tsRNA abundances measured by PANDORA-seq (C).

(D) tsRNA abundances (RPM) at L3 measured by mim-tsRNA-seq were correlated with published miRNA-seq data of 3rd-instar larvae (SRP048223 and SRP000602).

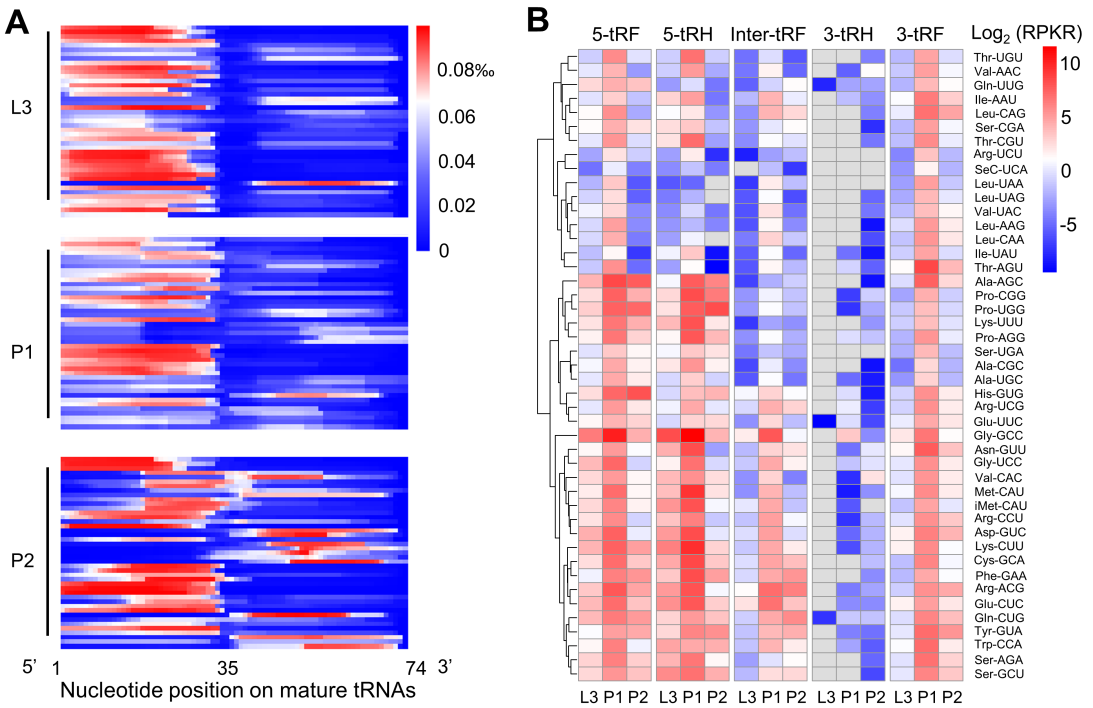

Supplemental Figure S3. Quantitative profiles of tRNA base coverage and tsRNA abundances from PANDORA-seq data

(A-B) Same as Figure 2B and 2E, respectively, but data were of PANDORA-seq.

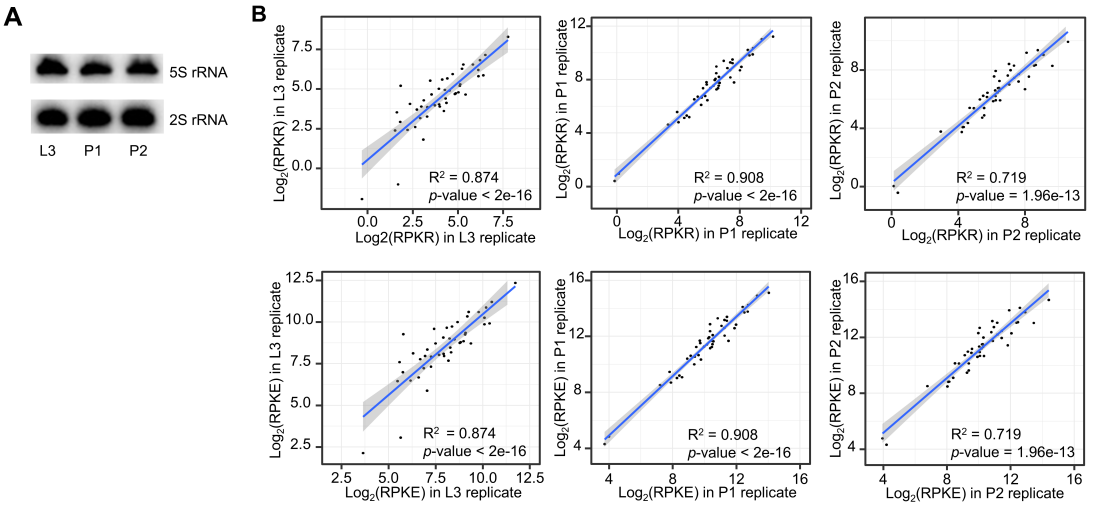

Supplemental Figure S4. Using 2S rRNA as an internal to quantify tsRNAs in mim-tsRNA-seq.

(A) Northern blot analyses against 5S and 2S rRNAs show stable expression during L3, P1 and P2 stages. For each lane, 5 μg of total RNA were used. Two independent experiments were performed with consistent results.

(B) Scatterplots showing high reproducibility of our tsRNA quantifications between biological replicates of each developmental stage. The tsRNA abundances were measured as either reads per kilo 2S rRNA-mapped reads (RPKR) or reads per kilo E. coli tRNA-mapped reads (RPKE). Coefficients of determination (R^2) were computed to evaluate the differences between replicates.

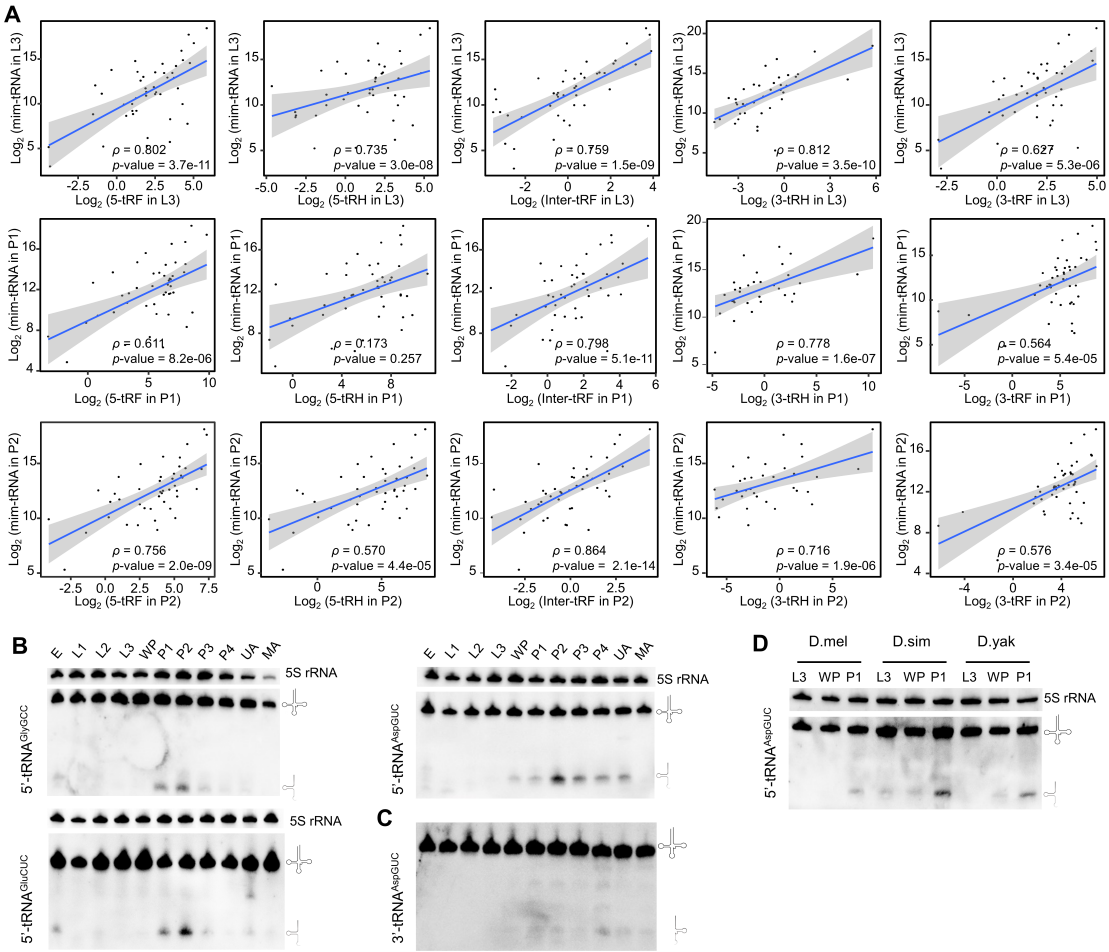

Supplemental Figure S5. 5'-tsRNAs prominently contribute to the increase in the overall tsRNA levels during the larva-to-pupa transition

(A) Scatterplots showing a reliable correlation between tsRNA and tRNA levels for each tsRNA subclass in each developmental stage.

(B) Northern blot analyses show the expression level of 5'-tsRNA^{AspGUC}, 5'-tsRNA^{GlyGCC} and 5'-tsRNA^{GluCUC} across 11 different developmental stages. E: embryos of 20~24 hours after deposition; L1-L2: 1st-2nd larvae; L3: wondering larvae; WP: white prepupae; P1-P3: pupae of 1-3 days after pupation; P4: pupae of >3 days after pupation; UA: unmated adults of virgin after eclosion; MA: mated adults of <4 days after eclosion. Each experiment (B-D) has two independent replicates with consistent results.

(C) Northern blot analyses against 3'-tsRNA^{Asp} across 11 different developmental stages.

(D) Northern blot analyses against 5'-tsRNA^{Asp} in L3, WP (white pupae) and P1 of *Drosophila melanogaster*, *Drosophila simulans* and *Drosophila yakuba*.

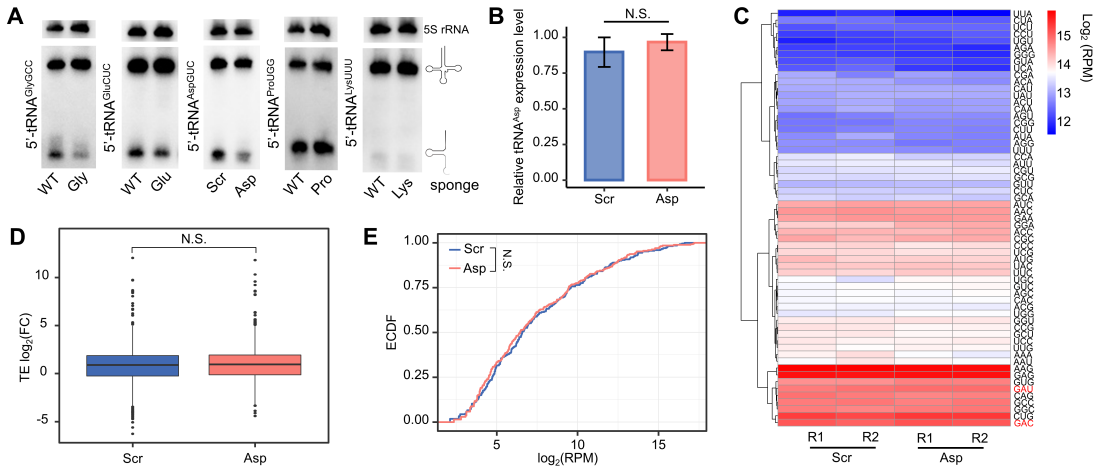

Supplemental Figure S6. The tRNA levels were not affected in *Tubulin*-GAL4-driven sponge pupae

(A) Northern blot analysis with 5' tRNA probes in WT control (w^{1118}) and *Tubulin*-GAL4>2×sponge lines (5'-tsRNA^{GlyGCC}, 5'-tsRNA^{GluCUC}, 5'-tsRNA^{ProUGG}, 5'-tsRNA^{AspGUC} and 5'-tsRNA^{LysUUU}) in early pupal stages. Each experiment has two independent replicates with consistent results.

(B) qRT-PCR confirming no significant difference (Student's *t*-test $p > 0.05$) in the tRNA^{AspGUC} level between *Tubulin*-GAL4>2×5'-tsRNA^{AspGUC} sponge and *Tubulin*-GAL4>2×5'-tsRNA^{AspGUC} scramble sponge. *rp49* mRNA was used as internal control.

(C) The heatmap profile of codon usage in A site, showing that the pattern of codons used in translation are not changed by the sponge element as a whole. Codons GAC and GAU for tRNA^{AspGUC} were marked in red.

(D) No significant difference in translation efficiency of 1,112 genes enriched with codons GAC/U between *Tubulin*-GAL4>2×5'-tsRNA^{AspGUC} sponge and *Tubulin*-GAL4>2×5'-tsRNA^{AspGUC} scramble sponge. Student's *t*-test $p = 0.09$.

(E) No significant difference in PANDORA-seq detected miRNAs and piRNAs. Kolmogorov–Smirnov test $p = 0.66$.

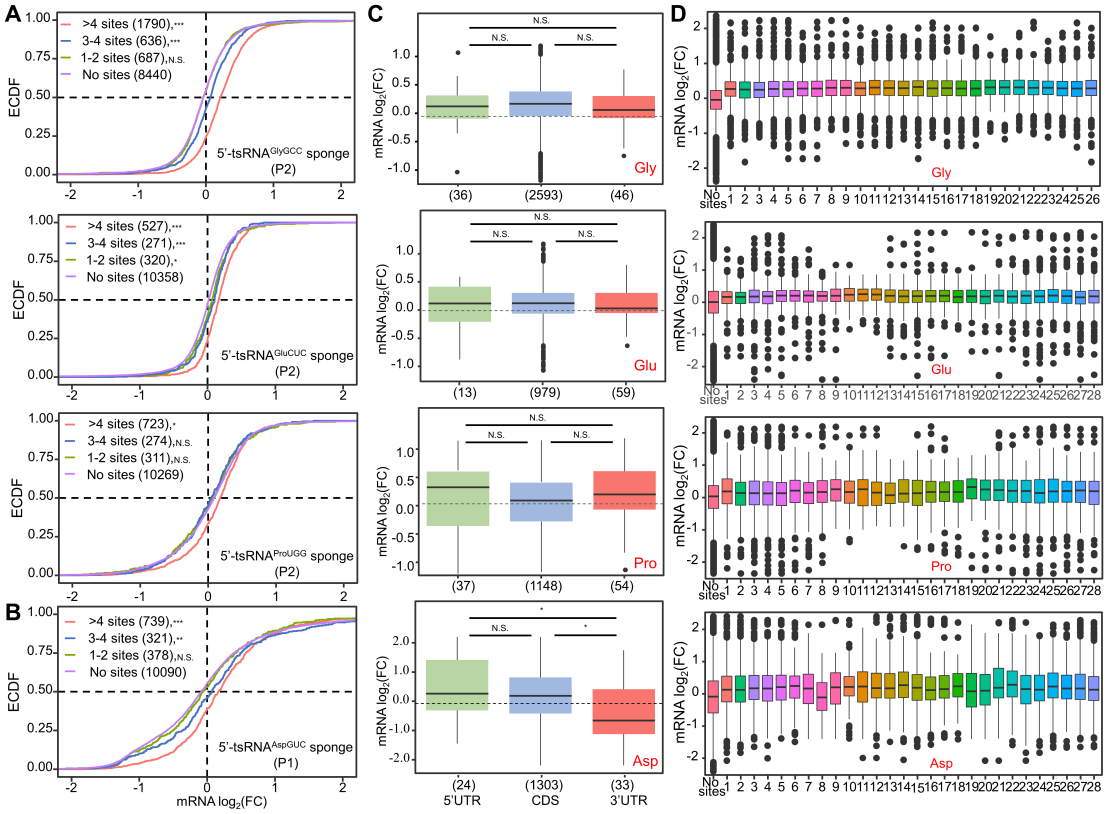

Supplemental Figure S7. Effective mRNA-level inhibition relies on the number of recognition sites without strict requirements of either mRNA site location or tsRNA seed selection

(A) Cumulative distribution of the fold differences in mRNA levels between each *Tubulin*-GAL4-driven sponge line and *Tubulin*-GAL4>2×5'-tsRNA^{LysUUU}-sponge at P2 stage.

(B) Cumulative distribution of the fold differences in mRNA levels between *Tubulin*-GAL4>2×5'-tsRNA^{AspGUC}-sponge and *Tubulin*-GAL4>2×scramble sponge at P1 stage.

(C) Shown are the fold differences in mRNA levels of genes carrying tsRNA target sites in only of the three regions: 5' UTR, CDS and 3' UTR. The dotted line represents the median value for genes without any predicted target sites of the corresponding tsRNA.

93 (D) Shown are the fold differences in mRNA levels of genes carrying tsRNA target sites

94 that are complementary to different seed positions along the corresponding tsRNA.

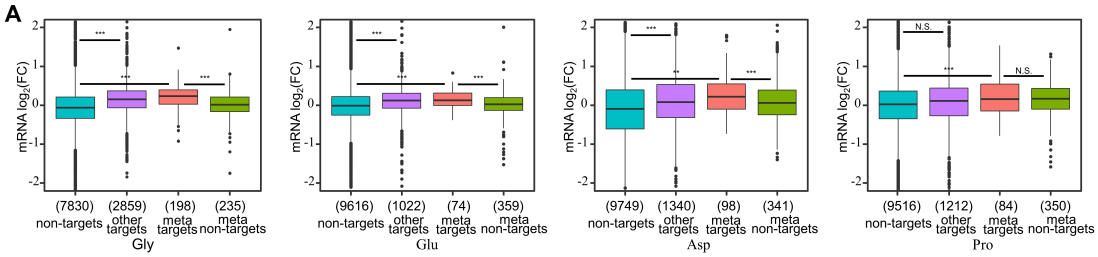

95

96 **Supplemental Figure S8. The tsRNA target genes in the metamorphosis pathway are**

97 **profoundly affected in the corresponding *Tubulin*-GAL4-driven sponge pupae.**

98 Student's *t*-tests were used.

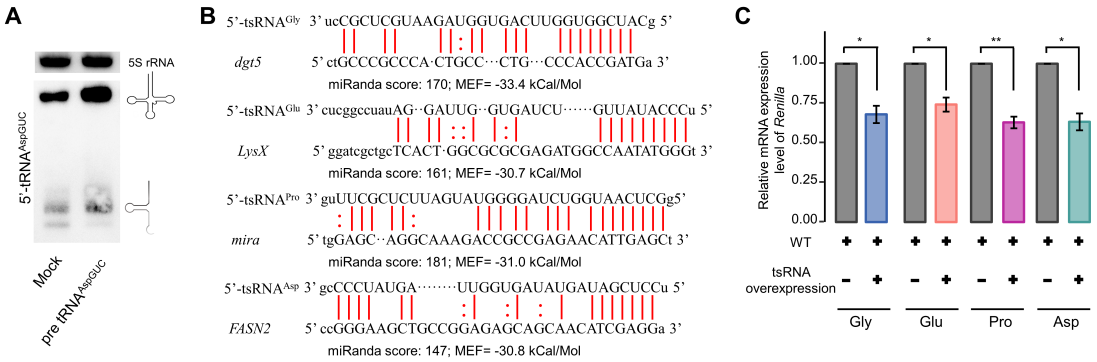

Supplemental Figure S9. Evaluation of 5'-tsRNAs' regulatory activities in S2 cells

(A) Northern blot analysis shows that expression of pre-tRNA^{AspGUC} could moderately increase 5'-tsRNA^{AspGUC} in S2 cells. Experiment has two independent replicates with consistent results.

(B) miRanda alignments between each target site used to construct the *Renilla* reporter gene and the corresponding tsRNA. See Table S5 for the respective sequences that were incorporated in the reporter gene.

(C) qRT-PCR confirming reduced mRNA levels of the *Renilla* reporter genes carrying the target sites under overexpression of the corresponding tsRNA. *Firefly* mRNA was used as internal control. Error bars represent SEM computed from two independent experiments.

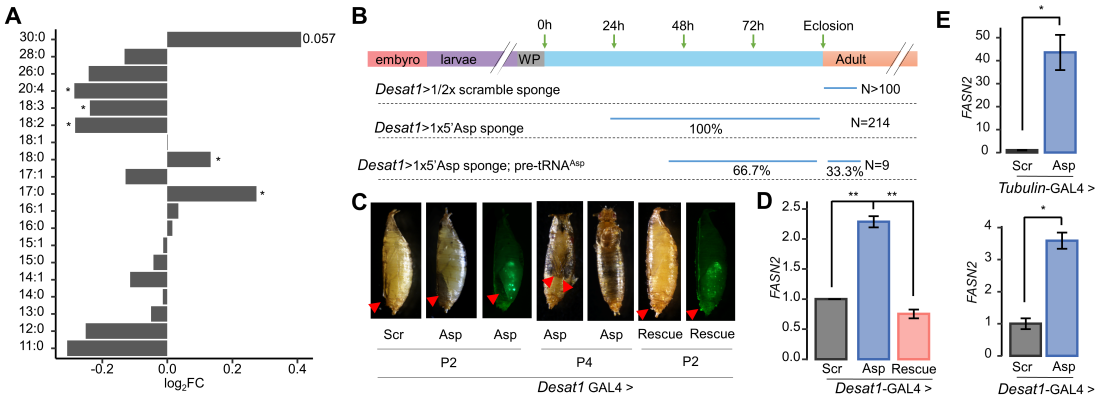

111

112 **Supplemental Figure S10. *FASN2* is an oenocyte-specific target of 5'-tsRNA^{AspGUC}**

113 (A) Fatty acids profile showing the fold differences between

114 *Tubulin*-GAL4>2×5'-tsRNA^{AspGUC}-sponge and *Tubulin*-GAL4>2×scramble sponge.

115 Samples were collected from P1 pupae. Each line has four independent experiments.

116 (B) Summary for the presumed lethality time of *Desat1*-GAL4-driven sponge lines.

117 (C) The pupal lethality phenotype of *Desat1*-GAL4>1×5'-tsRNA^{AspGUC}-sponge partially

118 rescued by 1×pre-tRNA^{AspGUC}. The sponge pupae ('Asp', N = 214) exhibited a

119 mis-localized bubble in ventral abdomen at P2, leg malformation at P4 and failure to

120 eclose. 1×pre-tRNA^{AspGUC} ('Rescue', N = 9) rescued the abdominal defect in all P2 pupae,

121 and 3 of them successfully emerged but died within the first day. Images of the GFP

122 channel confirm the oenocyte-specific expression during these stages.

123 (D) qRT-PCR confirmed that when driven by oenocyte-specific GAL4, the mRNA level of

124 *FASN2* was increased by 1×5'-tsRNA^{AspGUC} sponge and restored by 1×pre-tRNA^{AspGUC}.

125 Total RNA was extracted from whole-body samples of P2 pupae. Error bars represent

126 SEM computed from two independent experiments.

127 (E) Oenocyte-specific RiboTag mRNA-seq confirmed the increase of *FASN2* mRNA level

128 by 5'-tsRNA^{AspGUC} sponge. Top: bulk mRNA-seq difference between

129 *Tubulin*-GAL4>2×5'-tsRNA^{AspGUC}-sponge and *Tubulin*-GAL4>2×scramble sponge.

Bottom: RiboTag mRNA-seq difference between *Desat1*-GAL4>1×5'-tsRNA^{AspGUC}-sponge and *Desat1*-GAL4>1×scramble sponge. Error bars represent SEM computed from two independent experiments.

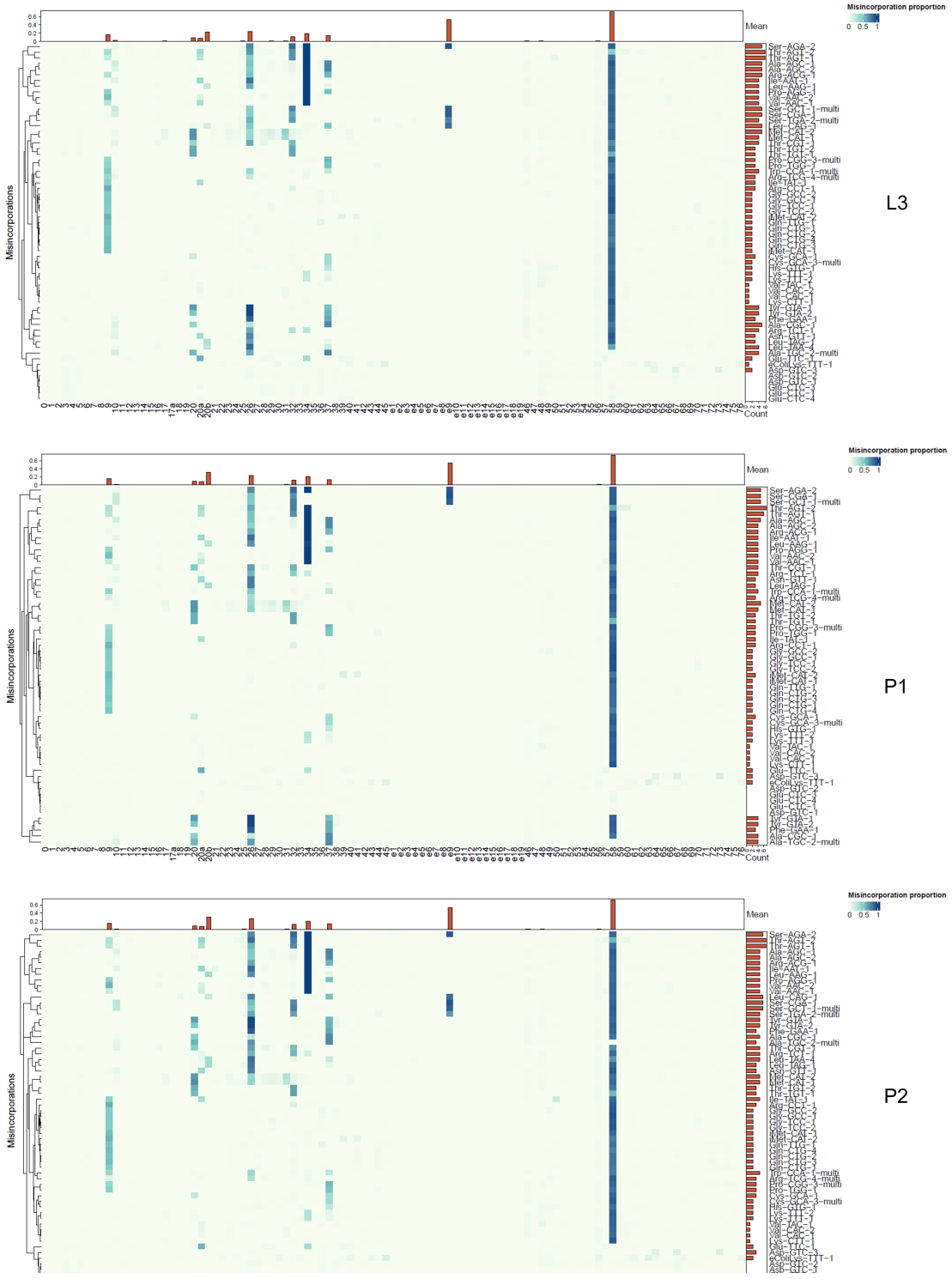

Supplemental Figure S11. Misincorporation mapping reveals no significant change in tRNA/tRNA modifications from L3 to P2 stage.

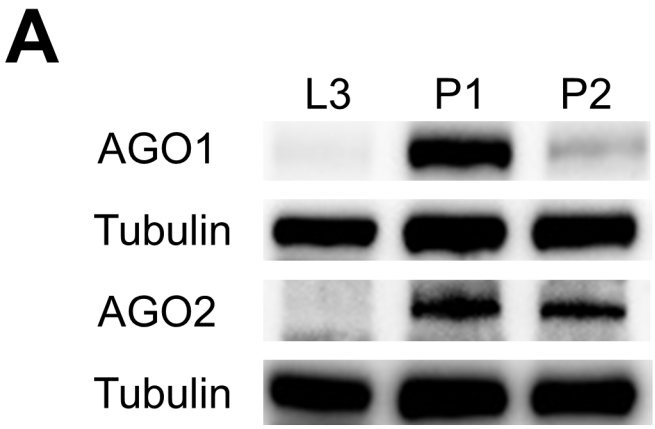

136

137 **Supplemental Figure S12. Western blot analysis showing the dynamic levels of AGO1**

138 **and AGO2 proteins at L3, P1 and P2 stages.** Each experiment has two independent

139 replicates with consistent results.